

Study on the Compensation of Silicon Photonics-Based Modulators in DCI Applications

Naim Ben-Hamida
Ciena Corporation
Ottawa, Canada
nbenhami@ciena.com

Ahmad Abdo
School of Electrical Engineering
and Computer Science
University of Ottawa
Ottawa, Canada
aabdo013@uottawa.ca

Xueyang Li,
Department of Electrical and
Computer Engineering
McGill University
Montreal, Canada
xueyang.li@mail.mcgill.ca

Md Samiul Alam,
Department of Electrical and
Computer Engineering,
McGill University
Montreal, Canada
md.samiul.alam@mail.mcgill.ca

Mahdi Parvizi
Ciena Corporation
Ottawa, Canada
mparvizi@ciena.com

Claude D'Amours
School of Electrical Engineering
and Computer Science
University of Ottawa
Ottawa, Canada
cdamours@uottawa.ca

David V. Plant
Department of Electrical and
Computer Engineering
McGill University
Montreal, Canada
david.plant@mcgill.ca

Abstract— For next generation high speed optical coherent systems, digital pre-emphasis filters are essential as they can pre-compensate for the transmitter frequency response and mitigate receiver noise enhancement. However, the downside of using full pre-emphasis to completely pre-compensate for the low bandwidth transmitter is that it increases the signal peak-to-average power ratio (PAPR), thus posing a higher effective number of bits (ENoB) requirement for the digital to analog converter (DAC) and increases optical modulation loss. In this paper, we study the impact of partial pre-emphasis filters on signal PAPR and show how partial pre-emphasis reduces DAC ENoB requirements and MZM modulation loss. Our proposed scheme reduced the DAC ENoB requirement from 5 to 4.5 bits at the same implementation SNR. This enables a lower optical module power through the reduction of DAC and driver amplifier (DA) power. The experimental results, for single-pol case for a partial pre-emphasis filter, showed that the system bandwidth can be extended from 10GHz to 20GHz and tolerate a 6dB loss for a 0.4dBQ penalty factor, and a 0.8dB PAPR reduction.

Keywords—Pre-emphasis, Optical Pluggable, Coherent Transceivers, Data-Center Interconnect, Silicon Photonics.

I. INTRODUCTION

Internet content providers face challenges of powering and cooling data centers. Due to these challenges, optical modem manufacturers are building prototypes based on the 400ZR standard [1]. The strategy of the DSP design of 400ZR represents a new paradigm in the coherent communication, as it is intended for data center interconnect (DCI) applications (up to 120 km) and with very low power to service the pluggable market in high-density form factors (such as QSFP-DD). The low cost and highly integrated solution provided by Silicon photonics (SiP) platform makes it an attractive choice in this perspective.

Silicon photonic traveling wave modulators (TWMZMs) have been actively studied and show good potential for coherent applications [2-8]. To meet the low power requirements in 400G SiP coherent systems, TWMZMs with low V_π are attractive, which allows for low power RF driver amplifiers (DA). However, this is obtained by trading off the modulator E-O bandwidth, which leads to the Tx low-pass filtering that is significantly stronger than the Rx [8]. Furthermore, the generation of the higher order modulation formats for coherent system and Nyquist pulse shaping requires the use of high-speed high resolution digital-to-analog converter (DAC) with sufficient 3dB electrical BW and resolution. This cascaded low-pass frequency response of the digital to analog converter (DAC) and modulator usually makes the Tx side quite band limited to operate with.

It is known that linear equalizers at the receiver can compensate for the frequency response of the entire channel including the severely band limited Tx, but also incur undesired noise enhancement. This can be mitigated by pre-compensating the Tx frequency response using a FIR pre-emphasis filter. In [9], adaptive pre-emphasis based on the common response of the receiver equalizers was proposed. The authors applied the method to optical fixed-grid applications with heavy filtering. Several works have been conducted on transmitter pre-emphasis targeting high speed coherent systems [10-13]. Authors in [10-11] proposed a pre-emphasis filter for the DAC frequency response, and in [12] the authors presented an adaptive digital pre-distortion (DPD) algorithm to mitigate the undesirable linear and non-linear distortions of the DAC, DA and MZM. However, pre-compensating for the entire Tx low-pass filtering leads to increased signal peak-to-average ratio (PAPR) and reduced average signal power out of the DAC, thus degrading the transmitter signal-to-noise-ratio (SNR).

In this paper, a lower signal PAPR is achieved and a higher signal power is obtained from the DAC when partial pre-

emphasis filter is used. First a numerical study showed the sensitivity of PAPR to pre-compensation for a 50 Gbaud 16QAM signal. It is found that the DAC effective number of bits (ENoB) requirement can be reduced by around 0.5 bits by using a partial pre-emphasis filter for the same transmitter signal SNR. Next, using discrete optical equipment, we experimentally characterize the overall performance penalty of partial pre-emphasis for a 50 Gbaud 16QAM short reach coherent system with extremely bandlimited Tx. The experimental results, for single-pol case for a partial pre-emphasis filter, showed that the system bandwidth can be extended to 20GHz and tolerate a 6dB loss for a 0.4dBQ penalty factor. The measurement setup involves a single-pol case system with Polarization-Dependent Loss (PDL) and Polarization-Dependent Dispersion (PMD) with a partial pre-emphasis. The proposed partial pre-emphasis filter can relieve ENoB requirement of the DAC, extend the effective bandwidth of the modulator, and reduce the total power of the coherent pluggable at the cost of a manageable performance penalty.

The paper is organized as follows: In section II, a study of a typical SiP MZM and its Electro-Optic (E-O) response is presented. In section III, PAPR sensitivity to Tx pre-compensation is highlighted through numerical study. Next, the experimental setup and DSP used to test the concept was described in section IV. Experimental results and discussion are presented in section V. Design trade-offs and engineering advantages of partial pre-emphasis are discussed in section VI.

II. SILICON-PHOTONICS IN SHORT REACH COHERENT APPLICATIONS

The silicon photonics (SiP) platform, among different platforms, is used to build optical transceivers targeting different reaches such as intra- and inter- datacenter ranging from 500 m to 120 km, metro-links, and even long-haul communications. This is attributed to the potential to build high volume, compact, high yield, high performance, and low cost complementary metal oxide semiconductor (CMOS) compatible devices. In the last decade, a plethora of SiP designs has been demonstrated including passive, active, and more complex photonic integrated circuits.

SiP modulators are used at the front-end of optical transponder to modulate a light beam produced by a tunable laser. The authors of this paper, in [2], investigated series push-pull modulator SiP MZM based ST fabrication process and fabricated in an SOI process with a low resistivity, Fig. 1. The length of the modulator transmission medium and the applied voltage bias determine the resulting frequency response (S21), Fig. 3. It was shown that the shorter the modulator, the higher the 3dB bandwidth when measured using small signal electro-optics (E-O) measurements. A common trade-off with the E-O bandwidth is the $V\pi$. A shorter modulator will have a higher E-O bandwidth due to reduced microwave losses, however, this will also have a larger $V\pi$ which will lead to a higher power driver. To counteract this bandwidth- $V\pi$ trade-off, methods of increasing the overlap between the optical wave and depletion region needs to be found [6].

In contrast to single-drive and series push-pull modulators (Fig. 1a), which have two electrical ports, one input and one

output, dual-drive modulators have four electrical ports, two inputs and two outputs, as depicted by Fig. 1b.

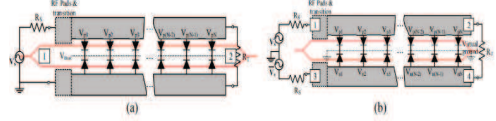


Fig. 1. Schematic of (a) series push-pull modulator which can be characterized by two ports, and (b) a dual-drive modulator which requires four port characterization. The dual-drive modulator shown here also has pn junction connected back-to-back and has a virtual ground at the middle due to its longitudinal symmetry. The red lines represent optical waveguides forming the MZMs.

The MZMs were fabricated on a silicon-on-insulator chip as part of a multi-project wafer run. The schematic of the cross-section of the process and the MZMs are shown in Fig. 2(a), and Fig. 2(b) and Fig. 2(c), respectively. The process had four copper metal layers with an aluminum cap layer. The waveguide rib height was 310 nm, and the slab was 163 nm thick. The buried oxide was 720nm thick.

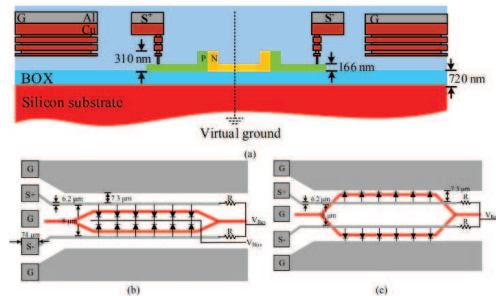


Fig. 2. (a) The cross-section of the SOI process with a dual-drive modulator. It also depicts the electrical wall and virtual ground at the middle of the device. (b) Schematic of a fabricated dual-drive modulator with diodes connected back-to-back in series and a common bias voltage node. (c) Schematic of a fabricated dual-drive modulator with diodes connected from the signal to ground electrodes.

The MZMs were designed with the pn junctions connected back-to-back, as shown in Fig. 2(b). Because these MZMs were differentially driven, no connections to ground were necessary. The ground signals improved isolation and offered additional control over the impedance. Devices with the pn junctions connected from the signal to ground lines, as shown in Fig. 2(c), were also fabricated. The signal traces were made in the top copper metal layer and the aluminum cap layer. The signal traces were 6.2 μm wide with an 8 μm spacing between them and 7.3 μm away from the ground traces. The RF signal pads were 74 \times 74 μm .

The MZM was driven by a GSGSG pad configuration, with the middle G being a dummy pad for the probe pin to land, as depicted in Fig. 2(b) and 2(c). The E-O frequency responses were measured with a Rohde & Schwarz ZVA67 four-port 67 GHz VNA with a true differential mode and a 50 GHz PD + TIA. The response of the PD + TIA was removed with the frequency response provided by the manufacturer. To maximize linearity, the MZMs were driven with a small signal and biased at quadrature. The fabricated devices also had a

contact node (VRes) at the middle of the terminations. This was probed and measured to be close to 0 V indicating that the devices were symmetrical and experimentally confirming the virtual ground. Moreover, the E-O responses measured from the devices of Fig. 2(b) and Fig. 2(c) were nearly identical, further validating that with differential drive there is no benefit in bandwidth of having the pn junction placed in series. The measured E-O responses are shown in Fig. 3. Because of the limited bandwidth of the MZM, RF drivers and DACs are used to pre-compensate the Tx transfer function and produce a flat frequency response.

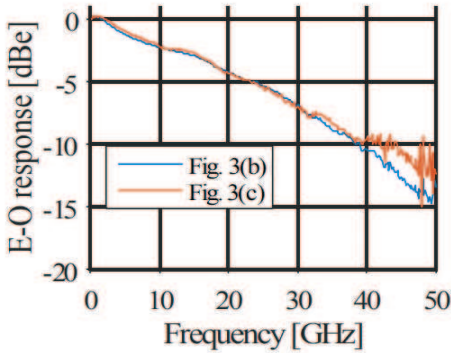


Fig. 3. Measured E-O responses of the configurations shown in Fig. 2(b), dual-drive modulator with diodes connected back-to-back in series, and Fig. 2(c), dual-drive modulator with diodes connected from the signal to ground electrodes.

III. PARTIAL PRE-EMPHASIS

Pre-emphasis filter is commonly used in optical communication systems to pre-compensate for part of or the entire channel ISI such that the noise enhancement associated with Rx equalization is alleviated. Nonetheless, the pre-emphasis filter applied to the signal at the Tx also burdens the DAC used to generate the RF signal due to increased signal PAPR. This leads to lower signal RMS, and equivalently lower signal power out from the DAC, thus degrading the signal SNR at the expense of quantization noise and distortion powers. In this section, we present a simulation model to investigate the impact of the pre-emphasis filter on the SNR of the signal at the output of the DAC.

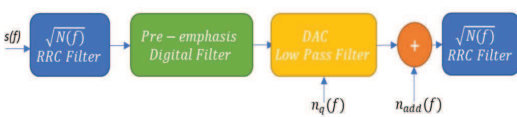


Fig. 4. Simulation Setup

Fig. 4. shows the simulation setup. The digital signal, $s(f)$ is generated and filtered by a Root Raised Cosine (RRC) pulse shaper, $\sqrt{N(f)}$, with a roll-off factor of 0.125, followed by a Digital Pre-emphasis filter (DPE). The DAC frequency response is modelled as a 3rd order Bessel filter with 14GHz of 3dB BW operating at 64 GSa/s. The quantization noise, $n_q(f)$ is

treated as Additive White Gaussian Noise with a variance of $\Delta^2/12$, where Δ is the quantization step size and depends on signal PAPR and ENoB. For the purpose of simplifying the comparison between different cases, we consider the nominal ENoB. An additional AWGN noise, $n_{add}(f)$ is added to better match to the practical DAC [19]. The DPE is calculated using Least Mean Square algorithm considering only the limited bandwidth of the DAC at the beginning and then used for all other results.

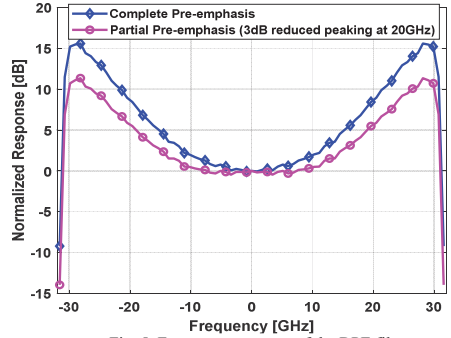


Fig. 5. Frequency response of the DPE filter

Fig. 5. shows the frequency response of the complete and partial-pre-emphasis filters created based on the full pre-emphasis filter. As can be seen in Fig. 5, there is a 3dB reduction of the frequency response at 20GHz for the partial pre-emphasis filter. In the rest of the simulation, the partial pre-emphasis filters are obtained by reducing the frequency response at 20GHz to different extent. As we stated earlier by doing the complete pre-emphasis, the signal PAPR increased which degraded the signal SNR at the output of the modulator.

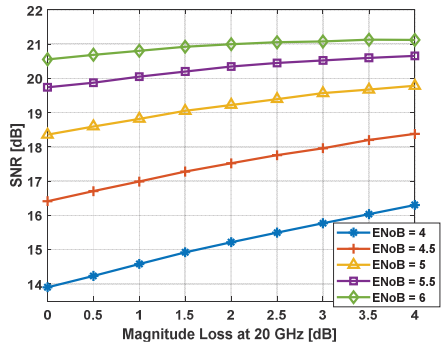


Fig. 6. Signal SNR vs Tx loss at 20GHz

Fig. 8 plots the PAPR of the transmitted signal into the DAC as a function of the magnitude loss at 20GHz. It is seen that the PAPR decreases almost linearly with the frequency loss and there is 1.3dB reduction of the PAPR for a 4dB loss at 20GHz. This reduction in PAPR increases the signal SNR.

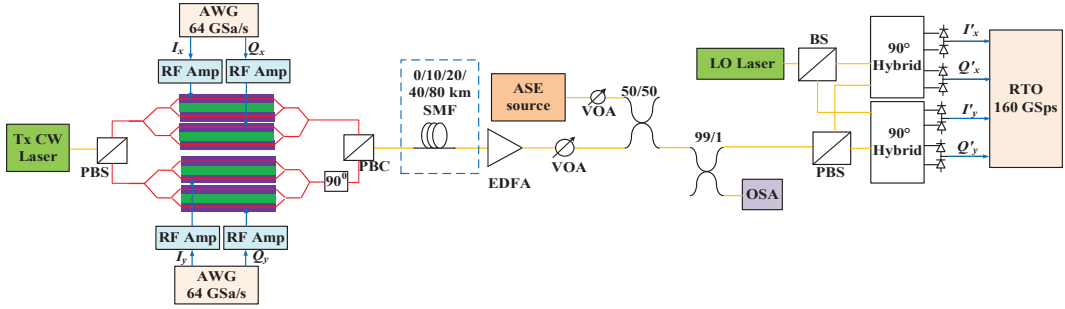


Fig. 7. Experimental setup

To calculate the transmitted signal SNR, we use a matched filter followed by an 11-tap feed-forward equalizer (FFE) at the receiver. The FFE removes the ISI caused by partial pre-emphasis. Fig. 6 plots the change of the signal SNR out of the DAC versus different losses at 20GHz when the ENoB varies from 4 to 6bits. It can be observed that the SNR increases with increasing loss for different ENoB values. This is a consequence of increasing the average signal power relative to the noise-plus-distortion power when the signal PAPR is reduced with increasing. This increase is more pronounced for lower ENoB values. With 4dB reduced peaking with ENoB of 4.5bits, we can get similar signal SNR as resulted from using an ENoB value of 5bits and complete pre-emphasis. This indicates that by applying partial pre-emphasis filters, the ENoB requirement of the DAC can be reduced such that lower power and cost coherent Tx can be built.

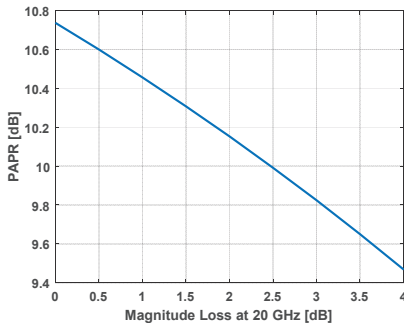


Fig. 8. PAPR vs Tx loss at 20 GHz

IV. EXPERIMENTAL SETUP AND DSP

Fig. 7 shows the experimental setup used to evaluate the impact of partial pre-emphasis. First, 16QAM symbols are generated in the Tx DSP and then resampled to the DAC sampling rate at 64GSa/s for pulse shaping via the root-raised-cosine (RRC) matched filter. Next, a pre-emphasis filter is applied to the signal to pre-compensate for the frequency response of the transmitter which has an overall 3dB bandwidth of 10GHz. Note that in the experiment, we reduce the peaking

of the pre-emphasis filter to different levels to achieve partial pre-emphasis of the Tx. Then, the signal is quantized and fed to the DAC memory for digital to analog conversion. The output RF signals from DAC are amplified by RF amplifiers with a 3dB bandwidth of 42GHz and a power gain of 26dB and then modulated onto the optical carrier at 1550.12 nm through an IQ modulator (IQM). In the setup, a LiNbO₃ IQM with a 3dB E-O bandwidth of 15GHz is used to emulate a low bandwidth SiP modulator. After transmission, the optical signal is pre-amplified and received by the coherent receiver (CRX). An ASE source along with a VOA is used to control the OSNR of the signal fed to this coherent receiver. The signal is then sampled by a 160GSa/s and 62GHz 3dB bandwidth two-channel real-time oscilloscope (RTO). The sampled signal is stored and processed following common coherent DSP algorithms, which includes resampling to 2 samples per symbol, frequency offset compensation, dispersion compensation, RRC matched filtering and PLL-interleaved equalization to compensate for both the ISI and the phase noise. Finally, the symbols are determined and decoded for BER calculation.

V. RESULTS AND DISCUSSION

The objective of the experimental results is to validate the numerical simulation and prove that the MZM bandwidth can be extended with minimum system penalty. This can be achieved by finding the optimum balance between Tx partial pre-emphasis and Rx post compensation filters. The optimization takes into consideration minimizing the DAC SNR and ENoB, Tx signal PAPR, and noise enhancement.

A. Impact of partial pre-compensation on Q-factor in a single-polarization coherent system

We first investigated the performance penalty of partial vs. full pre-compensation in a 50Gbaud 16QAM single-pol coherent system in back-to-back. Note that we used an extremely low bandwidth Tx chain (3dB BW of 10GHz) in the experiment to better study the impact of partial pre-compensation on the performance of a low cost, low power coherent system. Though this limits the system from working at 60Gbaud for 400ZR, the conclusion is still valid. Fig. 9 shows the Q factor penalty versus the partial pre-compensation measured as reduced frequency peaking at 20GHz obtained from experimental and numerical results.

Both simulation and measurement data show the Q factor penalty increases with increasing attenuation at 20GHz. The black (*) curve indicates in the experiment that a 0.4dB Q factor penalty occurs at 6dB attenuation at 20GHz. This is due to increased noise enhancement at the receiver since more Tx frequency response is compensated for by the receiver equalizer. The magenta (o) curve (right vertical axis) shows the PAPR of the RF signal into the modulator for different attenuation values at 20. Higher attenuation results in lower PAPR which will allow for the use of lower cost DACs with smaller ENoB and RF amplifiers with less stringent requirement on linearity, gain, and power. Measured reduction of PAPR is smaller than found simulation one, as we measure it after the DAC and DA, where low pass response of the Tx comes into play. We also measured the Q factor penalty associated with partial pre-emphasis for a 50Gbaud 16QAM transmission after 80 km on SSMF at different OSNR values. We found that the Q factor penalty increases from 0dB at 22dB OSNR to 0.11dB at 18dB OSNR for an attenuation of 3dB at 20GHz. It is worthwhile to note that though the PAPR of the received signal increases due to chromatic dispersion (CD), the Q factor penalty remains stable.

B. Impact of partial pre-compensation on Q-factor in a dual-polarization coherent system with PDL and PMD

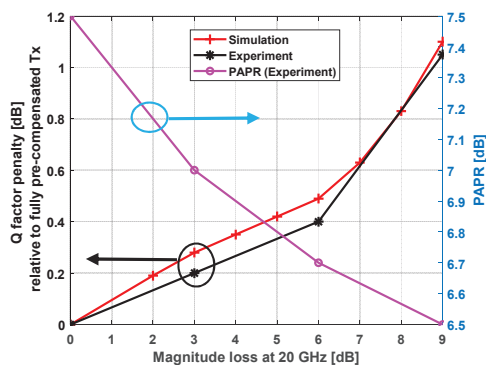


Fig. 9. Q-Factor penalty versus loss at high-frequency

Based on 400ZR specifications from [1], typical link impairments are expected to be handled by the adaptive filter at the Rx. In order to stress-test the Rx equalization capability so it performs further post-compensation while keeping the manageable Q penalty as shown in Fig. 9, we ran a dual-polarization experiment using the setup shown in Fig. 10. Using emulators, Polarization-Dependent Loss (PDL) of 3.5dB and Polarization-Mode Dispersion (PMD) of 28ps were set. PC1 and PC2 are used to scramble the signal polarization, emulating state-of-polarization (SOP) variations, at rotation rate of 1 rad/ms and 50 rad/ms, respectively. As well we included, as typically used in point-to-point DCI connections, a 75GHz C-Band Channel Mux/Demux (CMD) at the ingress and egress of the fiber model with a 3-dB net half bandwidth of 36GHz.

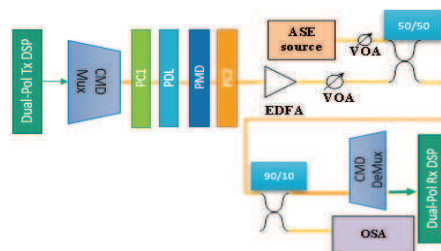


Fig. 10. Dual-polarization stress-test experimental setup

With a modulator attenuation at 20GHz equal to 3, 6 and 9dB, when comparing full versus partial pre-emphasis in presence of impairments, the Q-factor penalty is measured to be 0.25, 0.5, 1.1dB, respectively. In comparison to data presented in Fig. 9, the results show that adding impairments does not introduce more than 0.1dB of additional penalty.

VI. DESIGN TRADE-OFFS

An important aspect of 400ZR system design is power consumption. Reducing the frequency response peaking of the pre-emphasis filter, i.e. relying more on the post-compensation of the channel ISI, increases the signal power out from DAC, thus lessening the required gain of the driver or EDFA.

We summarize that partial pre-emphasis provides the following advantages for coherent system design at the expense of manageable performance penalty:

- This leads to less signal distortion from the nonlinearity of the RF DA and modulator due to reduced PAPR. It also helps mitigate the effect of fiber nonlinearity during transmission [20]. However, this has minimal performance impact on the targeted short-reach transmission, i.e. 100 km specified for 400ZR.
- It relaxes the “Adjacent channel isolation” per port specification for the channel Mux/DeMux (CMD) since for point-to-point fixed grid systems (i.e. 75GHz), partial pre-emphasis means that the inter channel interference will be mitigated due to less power leakage from adjacent channels. This also applies to gridless (or flexible-grid) coherent networks though not yet included in the 400ZR standard.
- Moreover, the fidelity of clock phase error estimators, such as Gardner [22] and Godard [23], that depends on the clean energy at the low and high end of the signal frequency response improves since partial pre-emphasis reduces the leaked noise into the edges of neighboring channels [24].

VII. CONCLUSION

In this work, we evaluate the impact of implementing partial pre-emphasis for low-cost, low-power short reach coherent systems. The numerical and experimental results indicate that partially pre-compensating for the Tx low-pass filtering leads to decreased signal PAPR, and this can help reduce the DAC ENoB requirement and extend the effective MZM BW. It is also found that the performance penalty due to partial pre-

emphasis is manageable for both single-pol and dual-pol coherent system.

REFERENCES

- [1] OIF, Implementation Agreement 400ZR, IA # OIF-400ZR 0.10-Draft, oif2017.245.10.pdf. [<https://www.oiforum.com/technical-work/hot-topics/400zr-2/>]
- [2] D. Patel et al., "Design, analysis, and transmission system performance of a 41 GHz silicon photonic modulator," *Opt. Exp.*, vol. 23, no. 11, pp. 14263-14287, 2015.
- [3] A. Samani et al., "A Low-Voltage 35-GHz Silicon Photonic Modulator-Enabled 112-Gb/s Transmission System," in *IEEE Photon. J.*, vol. 7, no. 3, pp. 1-13, 2015.
- [4] P. Dong, X. Chongjin, C. Long, L. L. Buhl, and YK Chen, "112-Gb/s monolithic PDM-QPSK modulator in silicon," *Opt. Exp.*, vol. 20, no. 26, pp. B624-B629, 2012.
- [5] J. Verbist et al., "A 40-GBd QPSK/16-QAM integrated silicon coherent receiver," *IEEE Photon. Technol. Lett.*, vol. 28, no. 19, pp. 2070-2073, 2016.
- [6] D. Patel, et al., "Frequency response of dual-drive silicon photonic modulators with coupling between electrodes," *Opt. Express* 26, 8904-8915 (2018)
- [7] C. Doerr et al., "Single-chip silicon photonics 100-Gb/s coherent transceiver," in *Proc. Opt. Fiber Commun. Conf.*, 2014, pp. Th5C.1.
- [8] D. Petousi et al., "Analysis of optical and electrical tradeoffs of traveling-wave depletion-type Si Mach-Zehnder modulators for high-speed operation," *IEEE J. Sel. Topics Quantum Electron.*, vol. 21, no. 4, pp. 199-206, 2014.
- [9] A. Abdo and C. Damours, "Adaptive Pre-Compensation of ROADMs in Coherent Optical Transponders," 2018 IEEE Canadian Conference on Electrical & Computer Engineering (CCECE), Quebec City, QC, 2018, pp. 1-4.
- [10] A. Napoli et al., "Novel DAC digital pre-emphasis algorithm for next generation flexible optical transponders," in *Proc. Opt. Fiber Commun. Conf.*, Los Angeles, CA, USA, 2015, pp. Th3G.6.
- [11] D. Rafique, A. Napoli, S. Calabro, and B. Spinnler, "Digital preemphasis in optical communication systems: On the DAC requirements for terabit transmission applications," in *J. Lightw. Technol.*, vol. 32, no. 19, pp. 3247-3256, Oct. 1, 2014.
- [12] G. Khanna et al. "A Robust Adaptive Pre-Distortion Method for Optical Communication Transmitter," in *IEEE Photon. Technol. Lett.*, vol. 28, no. 7, 752-755, 2015
- [13] D. Rafique, "Interplay of Pulse Shaping and Pre-Emphasis for High Symbol Rate Coherent Transmission Systems," 20th ICTON, IEEE, 2018.
- [14] Y. Kai et al., "130-Gbps DMT Transmission using Silicon Mach-Zehnder Modulator with Chirp Control at 1.55-um," in *Proc. Opt. Fiber Commun. Conf.*, 2015, Th4A.1.
- [15] M. Chagnon et al., "Experimental parametric study of a silicon photonic modulator enabled 112-Gbit/s PAM transmission system with a DAC and ADC", *J. lightwave technol.*, vol.33, no.7, p.1380, (2014).
- [16] C. E. Png, "Silicon-on-insulator phase modulators," PhD thesis, University of Surrey, 2004.
- [17] J. Teng, et al., "Athermal Silicon on-insulator ring resonators by overlaying a polymer cladding on narrowed waveguides," *Opt. Express*, vol. 17, pp. 14627 - 14633, 2009.
- [18] Jeison Tabares, "Digital Pre-emphasis for 10Gb/s with Low-cost Directly Phase-Modulated Lasers for PONs," *Advanced Photonics Congress*, 2018, pp. SpTh3G-2.
- [19] Napoli, Antonio, et al. "Digital compensation of bandwidth limitations for high-speed DACs and ADCs," *J. Lightw. Technol.*, vol. 34, no. 13, pp. 3053-3064, 2016.
- [20] M. Park, H. Jun, J. Cho, N. Cho, D. Hong and C. Kang, "PAPR Reduction in OFDM Transmission Using Hadamard Transform," *IEEE International Conference on Communications*, vol. 1, pp. 430-433, 2000.
- [21] C. Azeredo-Leme, "Clock Jitter Effects on Sampling: A Tutorial," in *IEEE Circuits and Systems Magazine*, vol. 11, no. 3, pp. 26-37, 2011.
- [22] F. Gardner, "A BPSK/QPSK timing-error detector for sampled receivers," *IEEE Trans. Commun.* vol. 34, no. 5, pp. 423-429, 1986,
- [23] D. Godard, "Passband Timing Recovery in an All-Digital Modem Receiver," in *IEEE Trans. Commun.* vol. 26, no. 5, pp. 517-523, 1978.
- [24] A. Abdo, S. Aouini, B. Riaz, B. N. Ben-Hamida and C. D'Amours, "Adaptive Coherent Receiver Settings for Optimum Channel Spacing in Gridless Optical Networks," *Future Internet* 2019, 11, 206.